Aortic Valve Stenosis and Aortic Diameters Determine the Extent of Increased Wall Shear Stress in Bicuspid Aortic Valve Disease

Emile S. Farag, MD,[1] Pim van Ooij, PhD,[2] R. Nils Planken, MD, PhD,[2] Kayleigh C.P. Dukker, MSc,[2] Frederiek de Heer, MSc,[1] Berto J. Bouma, MD, PhD,[3] Danielle Robbers-Visser, MD, PhD,[3] Maarten Groenink, MD, PhD,[2,3] Aart J. Nederveen, PhD,[2] Bas A.J.M. de Mol, MD, PhD,[1] Jolanda Kluin, MD, PhD,[1] and S. Matthijs Boekholdt, MD, PhD[3]*

Background: Use of 4-dimensional flow magnetic resonance imaging (4D-flow MRI) derived wall shear stress (WSS) heat maps enables identification of regions in the ascending aorta with increased WSS. These regions are subject to dysregulation of the extracellular matrix and elastic fiber degeneration, which is associated with aortic dilatation and dissection.
Purpose: To evaluate the effect of the presence of aortic valve stenosis and the aortic diameter on the peak WSS and surface area of increased WSS in the ascending aorta.
Study Type: Prospective.
Subjects: In all, 48 bicuspid aortic valve (BAV) patients (38.1 ± 12.4 years) and 25 age- and gender-matched healthy individuals.
Field Strength/Sequence: Time-resolved 3D phase contrast MRI with three-directional velocity encoding at 3.0T.
Assessment: Peak systolic velocity, WSS, and aortic diameters were assessed in the ascending aorta and 3D heat maps were used to identify regions with elevated WSS.
Statistical Tests: Comparisons between groups were performed by *t*-tests. Correlations were investigated by univariate and multivariate regression analysis.
Results: Elevated WSS was present in 15 ± 11% (range; 1–35%) of the surface area of the ascending aorta of BAV patients with aortic valve stenosis (AS) ($n = 10$) and in 6 ± 8% (range; 0–31%) of the ascending aorta of BAV patients without AS ($P = 0.005$). The mid-ascending aortic diameter negatively correlated with the peak ascending aortic WSS ($R = –0.413$, $P = 0.004$) and the surface area of elevated WSS ($R = –0.419$, $P = 0.003$). Multivariate linear regression analysis yielded that the height of peak WSS and the amount of elevated WSS depended individually on the presence of aortic valve stenosis and the diameter of the ascending aorta.
Data Conclusion: The extent of increased WSS in the ascending aorta of BAV patients depends on the presence of aortic valve stenosis and aortic dilatation and is most pronounced in the presence of AS and a nondilated ascending aorta.
Level of Evidence: 2
Technical Efficacy: Stage 2

J. MAGN. RESON. IMAGING 2018;48:522–530.

Bicuspid aortic valve (BAV) disease is the most common congenital cardiovascular anomaly, with an estimated prevalence of 1–2%.[1] Although patients are often asymptomatic, BAV is associated with an increased risk of aortic valve stenosis (AS) and progressive ascending aortic dilatation.[2] Follow-up typically consists of periodic

View this article online at wileyonlinelibrary.com. DOI: 10.1002/jmri.25956

Received Nov 22, 2017, Accepted for publication Jan 5, 2018.

*Address reprint requests to: S.M.B., Department of Cardiology, Academic Medical Center Amsterdam, P.O. Box 22660 - 1100 DD, Amsterdam, The Netherlands. E-mail: s.m.boekholdt@amc.uva.nl

From the [1]Department of Cardiothoracic Surgery, Academic Medical Center, Amsterdam, the Netherlands; [2]Department of Radiology, Academic Medical Center, Amsterdam, the Netherlands; and [3]Department of Cardiology, Academic Medical Center, Amsterdam, the Netherlands

This is an open access article under the terms of the Creative Commons Attribution-NonCommercial License, which permits use, distribution and reproduction in any medium, provided the original work is properly cited and is not used for commercial purposes.

 © 2018 The Authors Journal of Magnetic Resonance Imaging published by Wiley Periodicals, Inc. on behalf of International Society for Magnetic Resonance in Medicine

transthoracic echocardiography (TTE) to evaluate aortic valve morphology, diagnose aortic valve stenosis and/or regurgitation, as well as aortic diameters. Pressure gradients are calculated using the simplified Bernoulli equation and are used as a marker for aortic valve stenosis, but Doppler image acquisition is operator-dependent and can lead to over- or underestimation of hemodynamic parameters.[3] Furthermore, echocardiography and advanced imaging modalities (magnetic resonance imaging [MRI] or computed tomography) can be used to identify dilatation of the aortic root and ascending aorta, a risk factor for potentially fatal complications such as aortic dissection.[4,5]

Time-resolved 3D phase contrast MRI with three-directional velocity encoding, better known as 4D-flow MRI, allows for the quantification of blood velocity in both the heart and the great vessels. 4D-flow MRI measures volumetric velocity vector fields that can be used to calculate wall shear stress (WSS), a marker used to measure the viscous shear forces of flowing blood to the vessel wall.[6] Using patient-specific velocity and WSS heat maps, it is now possible to identify regions of increased velocity and WSS in individual BAV patients compared to age- and gender-matched healthy individuals.[7] A previous study has shown that BAV patients, both with and without valve dysfunction, exhibit increased peak WSS in the ascending aorta and that severe aortic valve regurgitation and/or stenosis causes increased WSS and exaggerated flow jet eccentricity.[8] Furthermore, a recent histological study found that areas subject to increased WSS are subject to dysregulation of the extracellular matrix and degeneration of elastic fibers in the aortic wall, leading to aortic wall remodeling.[9] Therefore, these regions are of specific interest, as identifying which patients are at high risk of aortic complications due to BAV disease may aid in the development of patient-specific treatment and follow-up strategies.

The clinical applicability of 4D-flow MRI has long been limited due to long scan times. However, in this study scan times were ~7 minutes, due to 8-fold undersampling and sparsity transform k-t principal component analysis reconstruction (kt-PCA), making this technique suitable for implementation in current clinical practice. We employed this clinically feasible 4D-flow MRI sequence in BAV patients to determine whether 1) the presence of aortic valve stenosis correlates with the amount of abnormal WSS in the aortic root and ascending aorta, 2) aortic diameters correlate with the amount of abnormal WSS, and 3) 4D-flow MRI-derived blood flow velocity values are comparable with those obtained with TTE.

Materials and Methods

Study Cohort

In a single-center prospective study, 48 adult (≥18 years) patients with BAV participated in this study between February 2016 and October 2016. Patients with contraindications for MRI or older than 65 years were not recruited for study participation. Demographic data, history of prior surgical cardiac or aortic interventions, and cardiovascular risk factors were obtained from electronic medical records. Twenty-five of the included 48 patients in this study had a history of surgical aortic coarctation (CoA) repair. Mean time after initial CoA repair was 29.3 ± 9.4 years. At the time of MRI, no patients were diagnosed with recoarctation by either echocardiography or contrast-enhanced magnetic resonance angiography (MRA). In addition, 25 healthy age- and gender-matched volunteers with no history of cardiovascular disease or surgery were enrolled. The Institutional Review Board approved the study and all patients provided signed informed consent.

Transthoracic Echocardiography (TTE)

Two-dimensional TTE was performed in all patients. A cardiologist (with 7 years of clinical experience) assessed aortic valve morphology, peak velocity, and mean and maximum pressure gradients. Furthermore, left ventricular enddiastolic and endsystolic diameters, ejection fraction, aortic valve area, Sievers classification of BAV, and the presence of aortic valve regurgitation were assessed. Gradation of AS was based on systolic peak velocities and/or mean pressure gradients measured using Doppler echocardiography (mild; between 2.5 and 3 m/s or mean gradient <20 mmHg, moderate; between 3 and 4 m/s or mean gradient 20–40 mmHg, severe; ≥4 m/s or mean gradient >40 mmHg).[3] Degree of aortic valve regurgitation (AR) was based on the width of the vena contracta, regurgitation jet width relative to LVOT diameter, pressure halftime, and the presence of diastolic flow reversal in the descending aorta.[10]

Contrast-Enhanced MRA

All patients underwent contrast-enhanced (CE)-MRA) as part of regular clinical follow-up to measure aortic dimensions. Aortic diameters were measured by a cardiovascular radiologist (with 14 years of clinical experience) at the level of the sinus of Valsalva, the sinotubular junction, the mid-ascending aorta, and at the brachiocephalic trunk. Dilatation of the ascending aorta was diagnosed if one or more segment diameters was greater than 40 mm.[2]

4D-Flow MRI

All patients and volunteers underwent cardiac and respiratory-gated sagittal 4D-flow MRI of the thoracic aorta on a 3.0T Ingenia scanner (Philips Healthcare, Best, the Netherlands). Parameters: spatio-temporal resolution: 2.5 × 2.5 × 2.5 mm^3, ±42 msec (24 timeframes); echo time, repetition time / flip angle (TE/TR/FA) = 2.1msec/3.4msec/8°; VENC: 150–250 cm/s; k-t PCA acceleration factor: 8.[11] The aorta was segmented (Mimics, Materialise, Leuven, Belgium) using 3D phase contrast MRA images, created by multiplication of the magnitude with the absolute velocity images followed by averaging over all timeframes. MRI data were corrected for eddy currents, Maxwell terms, and velocity aliasing using in-house software programmed in MatLab (MathWorks, Natick, MA). The peak systolic timeframe was defined as the timeframe with the highest velocity averaged over the segmentation. Peak aortic valve blood flow velocity in the ascending aorta was calculated at the peak systolic timeframe. Aortic WSS was

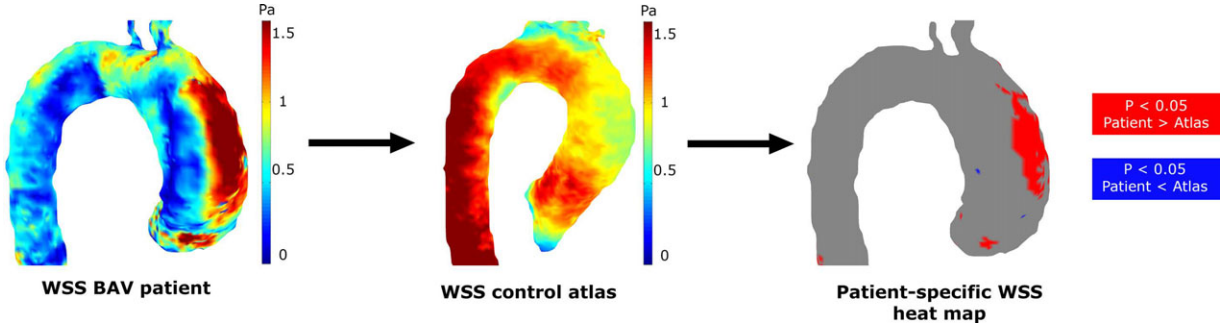

FIGURE 1: Individual patients peak systolic WSS maps are compared with peak systolic 3D WSS atlases, resulting in patient-specific WSS heat maps depicting regions with increased (red) or decreased (blue) WSS.

calculated with a previously published algorithm.[12] Mean WSS was calculated over the entire ascending aorta surface. Peak WSS was defined as the average of the highest 5% of WSS values in the ascending aorta, in order to eliminate the contribution of outliers. The ascending aorta was defined as the aorta between the aortic valve and the origin of the brachiocephalic trunk.

Cohort-averaged 3D velocity and WSS "heat maps" were created from the volunteer data, delineating elevated velocity and WSS in the aorta as previously described.[7] In short, a "shared" geometry of the control group was created. Each control was co-registered to the "shared" geometry, followed by interpolation of the peak systolic velocity and WSS values. After interpolation, the average and standard deviation (SD) of the velocity and WSS of the control cohort was calculated. Next, the average and SD velocity and WSS maps of the control cohort were projected onto the aortic geometry of each individual patient. By delineating in red where the velocity or WSS values of the patient were higher than the average +1.96*SD control values, and in blue where the velocity or WSS values of the patient were lower than the average –1.96*SD control values, velocity and WSS heat maps were created.

The amount of elevated WSS was expressed as the surface area with elevated WSS as a percentage of the entire surface area of the ascending aorta (Fig. 1). Finally, the heat maps were projected on cohort-specific "shared" geometries.[13] By addition of the heat maps, a 3D incidence map showing regional incidence of elevated velocity and WSS was created.

Statistical Analysis

Continuous variables with a normal distribution are reported as the mean ± SD and for between-group comparisons paired or unpaired *t*-tests were performed. Continuous variables with a non-normal distribution are reported as median (interquartile range), and were compared using the Mann–Whitney *U*-test. Results were tested for Gaussian distribution using the Kolmogorov–Smirnov test. Categorical variables are reported as number and percentage. The Fischer exact test was used to compare nominal variables. Correlations were investigated by univariate linear regression analysis and quantified by the correlation coefficient R. We used the Benjamini–Hochberg false discovery rate (FDR) method to control for an FDR of <12.5% in multiple comparisons, chosen to reflect the exploratory nature of the study. A multivariate linear regression model was used to assess the relationship of the presence of AS, maximum aortic diameter, age, and systolic blood pressure with the peak aortic WSS and the surface area of increased WSS in the ascending aorta. All four explanatory variables were included in an initial multivariate model, which was then optimized with manual backwards selection. For both peak aortic WSS and the surface area of increased WSS in the ascending aorta, the variables that could be removed from the multivariate model without affecting the significance were identified using a manual backwards selection process. For the multivariate model, the model that gave the minimum Akaike and Bayesian information criteria (AIC and BIC) was selected as the adequate model. All statistical tests were two-sided and a *P*-value of 0.05 or lower was considered statistically significant. Statistical analyses were performed using SPSS software for Mac OS X, v. 22.0 (Chicago, IL). GraphPad Prism 5.00 for Windows (GraphPad Software, La Jolla, CA) was used to create charts and graphs.

Results

Baseline Characteristics

In total, 48 BAV patients met the inclusion criteria and were included in this study. Baseline characteristics are summarized in Table 1. Ten patients had AS (mild; $n = 4$, moderate; $n = 4$, severe; $n = 2$). Two patients with AS also had AR ≥grade 2. Ten additional patients had AR ≥grade 2.

In 25 patients, BAV disease was present in combination with a history of CoA, all surgically treated during childhood and with no signs of recoarctation.

Furthermore, 25 age- (mean age 37,2 ± 13,2 years vs. 38.1 ± 12.4 years, $P = 0.77$) and gender-matched (9/25 women vs. 18/48 women, $P = 1.00$) healthy controls underwent 4D-flow MRI to compare WSS and velocity values between patients and healthy controls.

Bicuspid vs. Tricuspid Aortic Valves

In the overall study cohort, peak aortic valve blood flow velocities were significantly higher in BAV patients (2.11 ± 0.63 m/s) than in controls with a tricuspid aortic valve (TAV) (1.46 ± 0.48 m/s, $P < 0.001$). 4D-flow MRI-derived maximum aortic diameters were larger in BAV patients (40.5 ± 9.2 mm) than in TAV controls (31.3 ± 3.8 mm, $P < 0.001$). No differences were found between BAV patients and controls in peak ascending aortic WSS (BAV; 1.48 ± 0.49 Pa, TAV; 1.47 ± 0.41 Pa, $P = 0.90$) and mean ascending aortic WSS (BAV; 0.72 ± 0.22 Pa, TAV;

TABLE 1. Baseline Characteristics

	Cohort ($n = 48$, %)
Age, years	38.1 ± 12.4
Female	18 (37.5)
Body mass index, kg/m^2	24.0 ± 3.0
Body surface area, m^2	2.0 ± 0.2
Aortic valve stenosis	
No stenosis	38 (79)
Mild stenosis	4 (8)
Moderate stenosis	4 (8)
Severe stenosis	2 (4)
Aortic valve regurgitation	
No regurgitation	13 (27)
Mild regurgitation, grade 1	23 (48)
Moderate regurgitation, grade 2	11 (23)
Severe regurgitation, grade 3	1 (2)
Bicuspid aortic valve type	
Right-left cusp fusion	38 (79.2)
Right-non coronary cusp fusion	7 (14.6)
Left-non coronary cusp fusion	1 (2.1)
True bicuspid valve	2 (4.2)
Cardiovascular risk factors	
Hypertension	17 (35.4)
Diabetes mellitus	2 (4.2)
History of CoA repair	25 (52)

Data are presented as mean ± standard deviation or number (percentage).

0.73 ± 0.19 Pa, $P = 0.78$). Furthermore, no differences were found between various BAV types according to Sievers classification. Surface areas of elevated WSS in BAV patients ranged from 0–35%.

Aortic Valve Function

Peak aortic WSS was higher in patients with AS (1.90 ± 0.53 Pa) than in patients without AS (1.36 ± 0.42 Pa, $P = 0.003$) and TTE respectively 4D-flow MRI-derived peak aortic valve blood flow velocities both significantly correlated with peak ascending aortic WSS ($R = 0.308$, $P = 0.035$ vs. $R = 0.367$, $P = 0.010$). Mean aortic WSS was somewhat comparable between patients with (0.81 ± 0.21 Pa) and without AS (0.68 ± 0.21, $P = 0.108$). Elevated WSS was present in 15 ± 11% (range; 1–35%) of the surface area of the ascending aorta of BAV patients with AS and in 6 ± 8% (range; 0–31%) of the ascending aorta of BAV patients without AS ($P = 0.005$) and can be seen predominantly in the outer curvature of the ascending aorta (Fig. 2).

Peak aortic WSS (1.63 ± 0.69 Pa vs. 1.42 ± 0.41 Pa, $P = 0.352$) and mean WSS (0.70 ± 0.28 Pa vs. 0.71 ± 0.18 Pa, $P = 0.846$) did not differ between patients with vs. without AR ≥grade 2. Furthermore, no difference in the surface area of abnormal WSS was found between patients with (11 ± 13%) and without (7 ± 8 %, $P = 0.25$) AR ≥ grade 2.

Aortic Diameter

Mean aortic diameters in BAV patients were 33.7 ± 4.7 mm at the Sinus of Valsalva, 32.2 ± 5.6 mm at the sinotubular junction, 36.5 ± 6.8 mm in the mid-ascending aorta and 29.5 ± 4.8 mm at the brachiocephalic trunk. Aortic root and/or ascending aortic dilatation was diagnosed on CE-MRA in 17 patients. Differences between WSS distribution patterns are displayed in Fig. 3. The prevalence of aortic dilatation was similar among BAV patients with (3 of 10; 30%) vs. without AS (14 of 37; 38%, $P = 0.727$).

Peak WSS was significantly lower in patients with aortic dilatation (1.29 ± 0.55 Pa) than in patients without aortic dilatation (1.59 ± 0.43 Pa, $P = 0.038$). Also, mean WSS

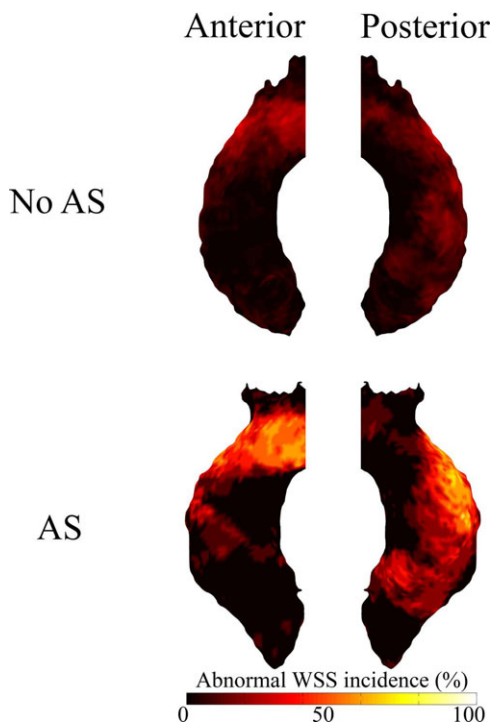

FIGURE 2: Incidence maps depicting the amount of patients (%) subject to increased WSS per region of the ascending aorta in patients with and without AS.

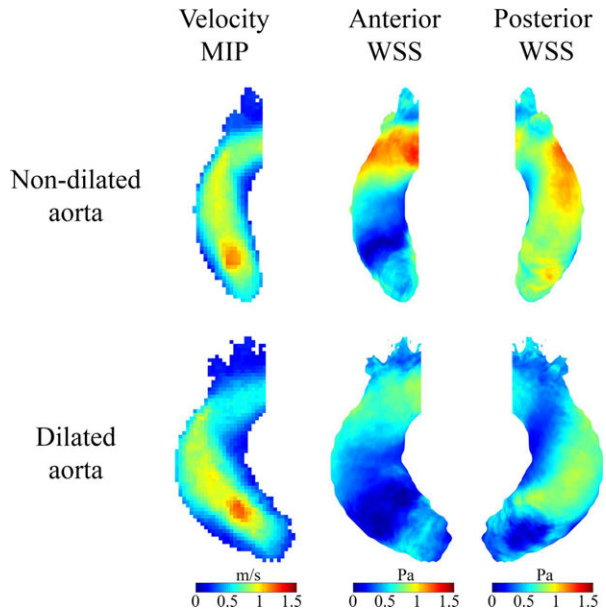

FIGURE 3: Cohort-averaged 3D maps for velocity and WSS for BAV patients with aortic dilatation (lower row) and without aortic dilatation (upper row) displayed in a shared geometry.

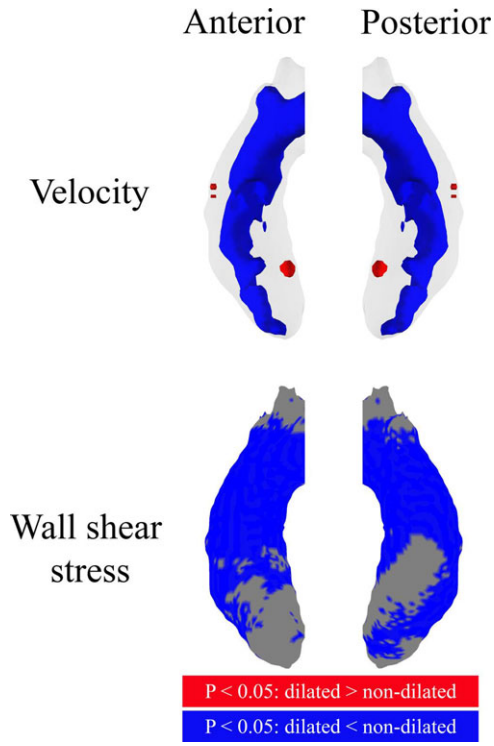

FIGURE 5: *P*-value maps displayed in a shared geometry of the ascending aorta from the anterior and posterior, displaying significant differences for velocity and WSS between patients with and without aortic dilatation. Red areas indicate significantly higher values for dilated aortas and blue areas for nondilated aortas.

was significantly lower in patients with aortic dilatation (0.55 ± 0.19 Pa) than in patients without aortic dilatation (0.81 ± 0.17 Pa, $P < 0.001$). The surface area of increased WSS was significantly lower in patients with ($4 \pm 7\%$) than in patients without aortic dilatation ($10 \pm 10\%$, $P = 0.038$). The mid-ascending aortic diameter negatively correlated with peak WSS ($R = -0.413$, $P = 0.004$) and the surface area of elevated WSS ($R = -0.419$, $P = 0.003$) (Fig. 4).

Per-voxel analysis using *P*-value maps (Fig. 5) shows that throughout the entire ascending aorta, central lumen velocities were lower in patients with aortic dilatation compared to patients without aortic dilatation. Furthermore, aortic WSS was significantly lower in large areas of the ascending aorta in BAV patients with vs. without aortic dilatation.

Agreement Between Transthoracic Echocardiography and 4D-Flow MRI

Time between TTE and MRI was in the range of −159 to +75 days. Peak velocities at the level of the aortic valve measured using TTE were compared with peak velocities at the vena contracta of the aortic valve measured using 4D-flow MRI. Bland–Altman comparison analysis revealed differences between both techniques with a mean difference of 0.023 ± 0.58 m/s and limits of agreement ranging from −1.12 to +1.16 m/s (Fig. 6).

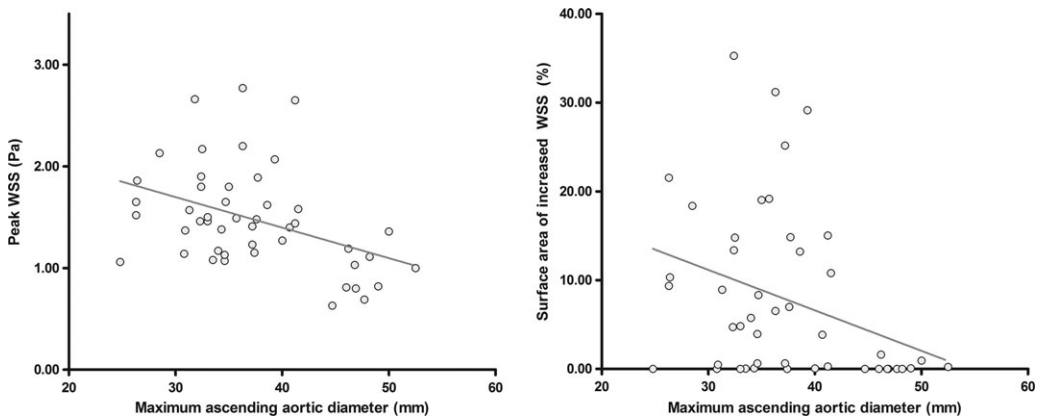

FIGURE 4: Significant correlations between the mid-ascending aortic diameter and peak WSS (left) and the surface area of increased WSS (right). The surface area of increased WSS (right) was lower than 5% in 26 BAV patients.

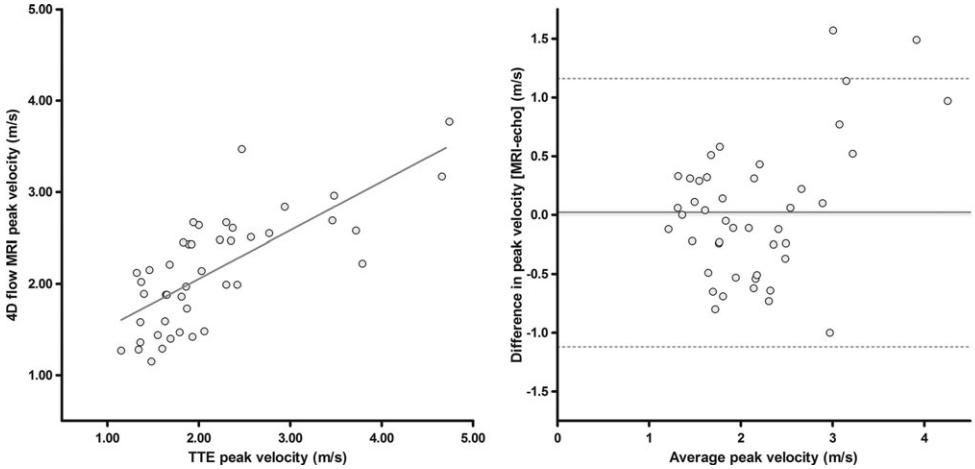

FIGURE 6: Orthogonal regression analysis (left) and Bland–Altman plot (right) of peak systolic blood flow velocities measured at the aortic valve with TTE and 4D-flow MRI.

History of Aortic Coarctation

CoA patients were significantly younger (34.2 ± 9.1 vs. 42.5 ± 14.3 years, $P = 0.022$), had significantly smaller ascending aortas (33.3 ± 4.6 vs. 41.3 ± 6.5 mm, $P < 0.001$) and lower peak aortic valve blood flow velocities (1.90 ± 0.56 vs. 2.42 ± 1.00 m/s, $P = 0.035$), but comparable systolic blood pressures (134 ± 19 vs. 131 ± 15 mmHg). As a result, mean and peak WSS were significantly higher in the ascending aorta, but surface areas of increased WSS were comparable to BAV patients with no history of CoA (Table 2).

Multivariate Prediction of Ascending Aortic WSS

Multivariate linear regression analysis was conducted to discover which variables were associated with peak ascending aortic WSS and with surface area of elevated WSS in the ascending aorta.

Peak ascending aortic WSS significantly increased in the presence of AS and higher systolic blood pressures and decreased as the maximum ascending aortic diameter increased. The surface area of elevated WSS also increased in the presence of AS and decreased as the maximum ascending aortic diameter increased (Table 3). Multivariate analysis showed that age did not contribute to the peak WSS and surface area of elevated WSS.

Discussion

In this series of patients with BAV disease, we employed 4D-flow MRI to quantify flow hemodynamics across the aortic valve and WSS in the ascending aorta. We utilized a kt-PCA sequence that is feasible in routine clinical practice because it can be performed in ~7 minutes. We observed reasonable agreement between peak aortic velocities as quantified by 4D-flow MRI and TTE. We found that the height of peak WSS and the amount of elevated WSS depend on the presence of aortic valve stenosis and the diameter of the ascending aorta.

It is well established that BAV patients have an increased risk of ascending aortic dilatation in comparison to patients with tricuspid aortic valves.[14,15] Current guidelines recommend preventive surgical replacement of the aortic root in BAV patients at a diameter of 5.0 cm or an aortic root growth rate of more than 2 mm per year, depending on the presence of additional risk factors.[4] However, current guidelines are subject to debate since they are based on absolute aortic dimensions and echocardiographic gradients as cutoff values and do not take individual patients' characteristics into consideration. Progressive ascending aortic dilatation in BAV patients occurs as a result of media degeneration of the aortic wall, which is thought to be caused by a combination of genetic predisposition in

TABLE 2. Comparison of Hemodynamic Parameters Between BAV Patients With and Without a History of CoA

	BAV only ($n = 23$)	BAV + CoA ($n = 25$)	*P*-value
Peak velocity (m/s)	2.31 ± 0.90	2.05 ± 0.78	0.285
Mean WSS (Pa)	0.61 ± 0.20	0.81 ± 0.19	0.001
Peak WSS (Pa)	1.29 ± 0.43	1.66 ± 0.49	0.009
Surface area of increased WSS (%)	4.52 ± 7.10	8.37 ± 9.42	0.120

TABLE 3. Uni- and Multivariate Analysis of Potential Risk Factors Associated With the Peak Aortic WSS and the Surface Area of Increased WSS in the Ascending Aorta

	Univariate analysis				Multivariate analysis			
		95% CI				95% CI		
	B	Lower	Upper	*P*-value	B	Lower	Upper	*P*-value
Peak WSS (Pa)								
Aortic stenosis	0.392	0.101	0.683	**0.008**	0.436	0.149	0.723	**0.003**
Max. aortic diameter	–0.023	–0.042	–0.004	**0.019**	–0.029	–0.045	–0.013	**<0.001**
Age	–0.007	–0.018	0.004	**0.220**	—	—	—	—
RR systolic	0.009	0.001	0.017	**0.021**	0.008	0.000	0.015	**0.046**
Surface area of increased WSS (%)								
Aortic stenosis	6.480	0.786	12.174	**0.026**	9.490	3.944	15.037	**0.001**
Max. aortic diameter	–0.400	–0.771	–0.029	**0.034**	–0.572	–0.908	–0.235	**0.001**
Age	–0.190	–0.405	0.025	**0.084**	—	—	—	—
RR systolic	0.176	0.026	0.325	**0.021**	—	—	—	—

BAV patients and abnormal blood flow patterns caused by BAV morphology.[16–18] By identifying patients who have large regions of altered WSS, we aim to identify which patients are at increased risk of aortic dilatation. A recent study focusing on peak systolic WSS found that increased WSS is present in BAV patients with comparable aortic diameters, regardless of aortic valve dysfunction.[8] It also showed that more severe aortic valve dysfunction resulted in a further increase of aortic WSS. However, peak WSS does not adequately predict BAV-related aortopathy, since it does not comprise the full extent of altered flow in the ascending aorta. Using the novel methodology to group patient-specific abnormal hemodynamics into regional incidence maps presented here, we provide a concise tool to investigate the pathological relationship between the extent of WSS and dilatation of the ascending aorta.

Our finding of a higher incidence of abnormal WSS in the BAV group with AS aligns with the idea that aortic valve dysfunction leads to increased WSS and finally results in degeneration of the aortic wall.[9,19] We found that increased WSS in BAV patients with AS occurs predominantly in the outer curvature of the ascending aorta, which is in accordance with clinical studies stating that aortic dilatation due to BAV disease occurs asymmetrically. In contrast, ascending aortic dilatation often occurs symmetrically in patients with tricuspid aortic valves.[20] The finding that the amount of elevated WSS is lower in aortas with higher diameters supports the hypothesis that aortic dilatation may be an adaptive process aimed at reducing WSS. Although velocity maximum intensity projections show comparable aortic flow jets, a wider aorta results in significantly lower velocity and WSS throughout the majority of the ascending aorta.

In a recent study, van Ooij et al hypothesized that aortic dilatation in BAV patients may be the result of different manifestations of aortic pathologies, with AS leading to outflow jets and subsequent eccentrically elevated WSS and aortic dilatation leading to helical flow and lower WSS values.[19] In our multivariate analysis, we indeed found that the presence of aortic valve stenosis and the peak ascending aortic diameter were independently associated with peak aortic WSS, supporting their hypothesis. Longitudinal and larger WSS cohort-averaged 3D and incidence maps studies may help to further clarify the mechanisms of abnormal flow and WSS that lead to vessel size regulation and wall remodeling in aortic valve disease.

Furthermore, in this study we compared ascending aortic blood flow between patients with isolated BAV and patients with BAV in combination with CoA. Frydrychowicz et al found that, compared to healthy volunteers, alterations in aortic hemodynamics after CoA repair were found in the entire thoracic aorta.[21] However, they did not correct for the presence of BAV (which was present in 12/28 patients, 43%) in their cohort. Among our BAV patients, we found higher mean and peak WSS values in the ascending aorta in CoA patients, but this did not result in an increased surface area of elevated WSS in the ascending aorta. All patients underwent surgical CoA repair before the age of 18, suggesting that ascending aortic blood flow after early CoA repair leads to WSS distribution in the ascending

aorta comparable to those of BAV patients without a history of CoA.

Finally, we compared peak blood flow velocities measured by 4D-flow MRI with TTE. Continuous wave Doppler TTE provides real-time imaging of the aortic valve, allowing for minimally invasive real-time measurements of blood flow velocities over the aortic valve. However, the accuracy of TTE measurements is highly dependent on the patient's acoustic windows and adequate beam orientation and gain settings.[3] We sought to expand on the potential utility of 4D-flow MRI in determining aortic valve function and found a statistically strong and significant correlation between TTE and 4D-flow MRI measured peak velocities. However, Bland–Altman comparison revealed that, at this point, both modalities cannot be used interchangeably. This finding is in accordance with recent studies conducted by other groups comparing 4D-flow MRI and TTE in a pediatric population, finding relatively large limits of agreement between both imaging techniques.[22] Differences between 4D-flow MRI and TTE may be explained by two factors. First, the relatively large voxel size ($2.5 \times 2.5 \times 2.5\,mm^3$) used in the acquisition of the 4D-flow MRI scan may result in underestimation of the peak velocity due to voxel dephasing, whereas echocardiography may result in underestimation due to misalignment of the measurement plane or poor acoustic windows.[23] Further 4D-flow MRI developments may allow for faster acquisition of data, making higher spatial resolutions possible, allowing for better 4D-flow MRI peak aortic valve pressure gradient assessment. Second, 4D-flow MRI scans and TTE scans were made in two different settings and in the majority of the cases on two different days. Hemodynamic factors, such as heart rate and blood pressure, can affect the evaluation of blood flow velocities and thus explain the differences between both diagnostic modalities.[24] This may result in significant over- or underestimation of 4D-flow MRI-derived peak velocity compared to TTE, as demonstrated in earlier studies in the aortic arch and carotid arteries.[21,25]

Limitations of this study are the relatively small number of patients who were included and the heterogeneity of the population with patients subject to various types of BAV morphology, aortic valve dysfunction, and aortic diameter. Nevertheless, our findings show a clear relationship between aortic valve function, aortic diameters, and the peak WSS and extent of increased WSS in the ascending aorta. During data acquisition, a respiratory navigator was placed on the lung–liver border to permit data acquisition during free breathing and was, if necessary, adjusted to achieve more efficient data collection. Both velocity and WSS values derived from 4D-flow MRI data have low interobserver and interstudy variability, as shown in a previous study.[26] Image quality was sufficient for analysis in every patient enrolled in this study. Additionally, the cross-sectional study design prohibits a prospective analysis of the effect of altered WSS on the ascending aortic growth rate. Follow-up studies will have to determine whether the degree and extent of aortic remodeling in BAV patients can be predicted using 4D-flow MRI and 4D-flow MRI derived WSS heat maps.

In conclusion, these findings indicate that 4D-flow MRI-derived 3D heat maps may offer additional information to magnetic resonance angiography and TTE, helping to identify which BAV patients are at risk of progressive aortic dilatation. Aortic valve stenosis and ascending aortic dimensions are associated with the amount of increased WSS in the ascending aorta and may aid in the identification of patients at risk of BAV-related aortic complications.

Conflict of Interest

The authors report no conflicts of interest.

References

1. Siu SC, Silversides CK. Bicuspid aortic valve disease. J Am Coll Cardiol 2010;55:2789–2800.
2. Erbel R, Aboyans V, Boileau C, et al. 2014 ESC guidelines on the diagnosis and treatment of aortic diseases. Eur Heart J 2014;35:2873–2926.
3. Baumgartner H, Hung J, Bermejo J, et al. Echocardiographic assessment of valve stenosis: EAE/ASE recommendations for clinical practice. Eur J Echocardiogr [Internet]. 2009 Jan 1 [cited 2017 Jul 3];10:1–25. Available from: http://www.ncbi.nlm.nih.gov/pubmed/19065003
4. Vahanian A, Alfieri O, Andreotti F, et al. Guidelines on the management of valvular heart disease (version 2012): The Joint Task Force on the Management of Valvular Heart Disease of the European Society of Cardiology (ESC) and the European Association for Cardio-Thoracic Surgery (EACTS). Eur J Cardiothoracic Surg [Internet]. 2012 Oct 1 [cited 2017 Mar 29];42:S1–44. Available from: https://academic.oup.com/ejcts/article-lookup/doi/10.1093/ejcts/ezs455
5. Tanaka R, Yoshioka K, Niinuma H, Ohsawa S, Okabayashi H, Ehara S. Diagnostic value of cardiac CT in the evaluation of bicuspid aortic stenosis: Comparison with echocardiography and operative findings. Am J Roentgenol 2010;195:895–899.
6. Dyverfeldt P, Bissell M, Barker AJ, et al. 4D-flow cardiovascular magnetic resonance consensus statement. J Cardiovasc Magn Reson [Internet]. 2015;17:72. Available from: http://jcmr-online.com/content/17/1/72
7. van Ooij P, Potters WV, Collins J, et al. Characterization of abnormal wall shear stress using 4D-flow MRI in human bicuspid aortopathy. Ann Biomed Eng [Internet]. 2015;43:1385–1397. Available from: http://www.ncbi.nlm.nih.gov/pubmed/25118671
8. Shan Y, Li J, Wang Y, et al. Aortic shear stress in patients with bicuspid aortic valve with stenosis and insufficiency. J Thorac Cardiovasc Surg [Internet]. 2017 Feb 10 [cited 2017 Mar 29];153:1263–1272.e1. Available from: http://linkinghub.elsevier.com/retrieve/pii/S0022522317301915
9. Guzzardi DG, Barker AJ, Van Ooij P, et al. Valve-related hemodynamics mediate human bicuspid aortopathy: insights from wall shear stress mapping. J Am Coll Cardiol 2015;66:892–900.
10. Nishimura RA, Otto CM, Bonow RO, et al. 2014 AHA/ACC guideline for the management of patients with valvular heart disease: A report of the American College of Cardiology/American Heart Association task force on practice guidelines [Internet]. Vol. 63, J Am Coll Cardiol 2014 [cited 2017 Mar 29]. Available from: http://www.sciencedirect.com/science/article/pii/S0735109714012790

11. Pedersen H, Kozerke S, Ringgaard S, Nehrke K, Won YK. K-t PCA: Temporally constrained k-t BLAST reconstruction using principal component analysis. Magn Reson Med 2009;62:706–716.

12. Potters WV, Van Ooij P, Marquering H, VanBavel E, Nederveen AJ. Volumetric arterial wall shear stress calculation based on cine phase contrast MRI. J Magn Reson Imaging 2015;41:505–516.

13. Van Ooij P, Potters WV, Nederveen AJ, et al. A methodology to detect abnormal relative wall shear stress on the full surface of the thoracic aorta using four-dimensional flow MRI. Magn Reson Med [Internet]. 2015 Mar 1 [cited 2017 Jun 16];73:1216–1227. Available from: http://doi.wiley.com/10.1002/mrm.25224

14. Tadros TM, Klein MD, Shapira OM. Ascending aortic dilatation associated with bicuspid aortic valve. Pathophysiology, molecular biology, and clinical implications. Circulation [Internet]. 2009 [cited 2017 Mar 29];119:880–890. Available from: http://www.ncbi.nlm.nih.gov/entrez/query.fcgi?cmd=Retrieve&db=PubMed&dopt=Citation&list_uids=19221231%5Cnhttp://circ.ahajournals.org/cgi/reprint/119/6/880.pdf

15. Cecconi M, Nistri S, Quarti A, et al. Aortic dilatation in patients with bicuspid aortic valve. J Cardiovasc Med [Internet]. 2006 May 15 [cited 2017 Mar 29];7:11–20. Available from: http://content.wkhealth.com/linkback/openurl?sid=WKPTLP:landingpage&an=01244665-200601000-00005

16. Russo CF, Cannata A, Lanfranconi M, Vitali E, Garatti A, Bonacina E. Is aortic wall degeneration related to bicuspid aortic valve anatomy in patients with valvular disease? J Thorac Cardiovasc Surg [Internet]. 2008 Oct [cited 2017 Mar 30];136:937–942. Available from: http://linkinghub.elsevier.com/retrieve/pii/S0022522308010660

17. Tang PCY, Coady MA, Lovoulos C, et al. Hyperplastic cellular remodeling of the media in ascending thoracic aortic aneurysms. Circulation [Internet]. 2005 Aug 23 [cited 2017 Mar 30];112:1098–10105. Available from: http://www.ncbi.nlm.nih.gov/pubmed/16116068

18. Fedak PWM, Verma S, David TE, Leask RL, Weisel RD, Butany J. Clinical and pathophysiological implications of a bicuspid aortic valve. Circulation [Internet]. 2002 Aug 20 [cited 2017 Mar 30];106:900–904. Available from: http://www.ncbi.nlm.nih.gov/pubmed/12186790

19. van Ooij P, Markl M, Collins JD, et al. Aortic valve stenosis alters expression of regional aortic wall shear stress: New insights from a 4-dimensional flow magnetic resonance imaging study of 571 subjects. J Am Heart Assoc [Internet]. 2017 Sep 13 [cited 2017 Oct 27];6:e005959. Available from: http://www.ncbi.nlm.nih.gov/pubmed/28903936

20. Tsamis A, Phillippi JA, Koch RG, et al. Extracellular matrix fiber microarchitecture is region-specific in bicuspid aortic valve-associated ascending aortopathy. J Thorac Cardiovasc Surg [Internet]. 2016 Jun [cited 2017 Jul 6];151:1718–1728. Available from: http://linkinghub.elsevier.com/retrieve/pii/S0022522316002385

21. Frydrychowicz A, Markl M, Hirtler D, et al. Aortic hemodynamics in patients with and without repair of aortic coarctation. Invest Radiol [Internet]. 2011;46:1. Available from: http://content.wkhealth.com/linkback/openurl?sid=WKPTLP:landingpage&an=00004424-900000000-99755

22. Gabbour M, Rigsby C, Markl M, et al. Comparison of 4D-flow and 2D PC MRI blood flow quantification in children and young adults with congenital heart disease. J Cardiovasc Magn Reson [Internet]. 2013;15:E90. Available from: http://jcmr-online.biomedcentral.com/articles/10.1186/1532-429X-15-S1-E90

23. Baumgartner H, Hung J, Bermejo J, et al. Echocardiographic assessment of valve stenosis: EAE/ASE recommendations for clinical practice. Eur J Echocardiogr [Internet]. 2009 Jan 1 [cited 2017 Dec 7];10:1–25. Available from: http://www.ncbi.nlm.nih.gov/pubmed/19065003

24. Little SH, Chan K-L, Burwash IG. Impact of blood pressure on the Doppler echocardiographic assessment of severity of aortic stenosis. Heart [Internet]. 2007 Jul [cited 2017 Jul 17];93:848–855. Available from: http://heart.bmj.com/lookup/doi/10.1136/hrt.2006.098392

25. Harloff A, Zech T, Wegent F, Strecker C, Weiller C, Markl M. Comparison of blood flow velocity quantification by 4D-flow MR imaging with ultrasound at the carotid bifurcation. [cited 2017 Dec 12]; Available from: http://www.ajnr.org/content/ajnr/early/2013/02/21/ajnr.A3419.full.pdf

26. Van Ooij P, Powell AL, Potters WV, Carr JC, Markl M, Barker AAJ. Reproducibility and interobserver variability of systolic blood flow velocity and 3D wall shear stress derived from 4D-flow MRI in the healthy aorta. J Magn Reson Imaging [Internet]. 2016 Jan [cited 2017 Aug 16];43:236–248. Available from: http://www.ncbi.nlm.nih.gov/pubmed/26140480